PHYSICAL REVIEW C **96**, 011301(R) (2017)

Triaxiality of neutron-rich ^{84,86,88}Ge from low-energy nuclear spectra

M. Lettmann,[1,*] V. Werner,[1] N. Pietralla,[1] P. Doornenbal,[2] A. Obertelli,[2,3] T. R. Rodríguez,[4] K. Sieja,[5] G. Authelet,[3] H. Baba,[2] D. Calvet,[3] F. Château,[3] S. Chen,[2,6] A. Corsi,[3] A. Delbart,[3] J.-M. Gheller,[3] A. Giganon,[3] A. Gillibert,[3] V. Lapoux,[3] T. Motobayashi,[2] M. Niikura,[7] N. Paul,[2,3] J.-Y. Roussé,[3] H. Sakurai,[2,7] C. Santamaria,[3] D. Steppenbeck,[2] R. Taniuchi,[2,7] T. Uesaka,[2] T. Ando,[2,7] T. Arici,[8] A. Blazhev,[9] F. Browne,[10] A. Bruce,[10] R. J. Caroll,[11] L. X. Chung,[12] M. L. Cortés,[1,2,8] M. Dewald,[9] B. Ding,[13] F. Flavigny,[14] S. Franchoo,[14] M. Górska,[8] A. Gottardo,[14] A. Jungclaus,[15] J. Lee,[16] B. D. Linh,[12] J. Liu,[16] Z. Liu,[13] C. Lizarazo,[1,8] S. Momiyama,[2,7] K. Moschner,[9] S. Nagamine,[7] N. Nakatsuka,[17] C. Nita,[18] C. R. Nobs,[10] L. Olivier,[14] Z. Patel,[11] Zs. Podolyák,[11] M. Rudigier,[11] T. Saito,[7] C. Shand,[11] P.-A. Söderström,[1,2,8] I. Stefan,[14] V. Vaquero,[15] K. Wimmer,[7] and Z. Xu[16,19]

[1]*Institut für Kernphysik, Technische Universität Darmstadt, 64289 Darmstadt, Germany*
[2]*RIKEN Nishina Center, 2-1 Hirosawa, Wako, Saitama 351-0198, Japan*
[3]*CEA, Centre de Saclay, IRFU/Service de Physique Nucléaire, 91191 Gif-sur-Yvette, France*
[4]*Departamento de Física Teórica, Universidad Autónoma de Madrid, 28049 Madrid, Spain*
[5]*IPHC, CNRS/IN2P3 et Université de Strasbourg, 67037 Strasbourg, France*
[6]*State Key Laboratory of Nuclear Physics and Technology, Peking University, Beijing 100871, People's Republic of China*
[7]*Department of Physics, University of Tokyo, 7-3-1 Hongo, Bunkyo, Tokyo 113-0033, Japan*
[8]*GSI Helmholtzzentrum für Schwerionenforschung GmbH, 64291 Darmstadt, Germany*
[9]*Institut für Kernphysik, Universität zu Köln, 50937 Köln, Germany*
[10]*School of Computing Engineering and Mathematics, University of Brighton, Brighton BN2 4GJ, United Kingdom*
[11]*Department of Physics, University of Surrey, Guildford GU2 7XH, United Kingdom*
[12]*Institute for Nuclear Science and Technology, VINATOM, P.O. Box 5T-160, Nghia Do, Hanoi, Vietnam*
[13]*Institute of Modern Physics, Chinese Academy of Sciences, Lanzhou 730000, People's Republic of China*
[14]*Institut de Physique Nucléaire Orsay, IN2P3-CNRS, 91406 Orsay Cedex, France*
[15]*Instituto de Estructura de la Materia, CSIC, 28006 Madrid, Spain*
[16]*Department of Physics, University of Hong Kong, Pokfulam, Hong Kong*
[17]*Department of Physics, Faculty of Science, Kyoto University, Kyoto 606-8502, Japan*
[18]*Horia Hulubei National Institute of Physics and Nuclear Engineering (IFIN-HH), 077125 Bucharest, Romania*
[19]*KU Leuven, Instituut voor Kern- en Stralingsfysica, 3001 Leuven, Belgium*

(Received 3 February 2017; published 5 July 2017)

γ-ray transitions between low-spin states of the neutron-rich ^{84,86,88}Ge were measured by means of in-flight γ-ray spectroscopy at 270 MeV/u. Excited 6_1^+, $4_{1,2}^+$, and $2_{1,2}^+$ states of ^{84,86}Ge and 4_1^+ and $2_{1,2}^+$ states of ^{88}Ge were observed. Furthermore, a candidate for a 3_1^+ state of ^{86}Ge was identified. This state plays a key role in the discussion of ground-state triaxiality of ^{86}Ge, along with other features of its low-energy level scheme. A new region of triaxially deformed nuclei is proposed in the Ge isotopic chain.

DOI: 10.1103/PhysRevC.96.011301

Since the early days of nuclear structure physics, nuclei of triaxial shape have been a subject of high interest. In the 1950s, two elementary models were derived, which include a breaking of the axial symmetry of the Bohr Hamiltonian [1] by introducing the triaxial deformation parameter γ in addition to the ellipsoidal elongation β. The γ parameter ranges from 0° (prolate shape) to 60° (oblate shape), and maximum triaxiality occurs at 30°. The rigid triaxial rotor model by Davydov and Filippov [2] considers a well-defined minimum for a certain value of γ in the potential energy surface while the model by Wilets and Jean [3] treats the potential independently of γ, called γ soft. More microscopic models, such as the shell model [4,5], the algebraic interacting boson model (IBM) [6], mean field approaches (e.g., Ref. [7]), or energy density functional–based models (e.g., Ref. [8]), discuss potential energy surfaces in terms of the geometrical deformation parameters β and γ.

The discussion of triaxiality in nuclei covers various regimes of angular momenta. At high spins, quasiparticle configurations or so-called wobbling modes (e.g., Refs. [9–11]) have been found to be the basis of triaxial superdeformed bands. At intermediate spins, there has been much discussion about chirality in odd-odd and even-Z nuclei [12–15], based on the spin axes of the unpaired proton and neutron and the rotational axis of the core. However, in this regime, in some cases there has been controversy as to the rigidity or softness of the nuclear body leading to the observed structures [16]. At the lowest spins, however, especially in the ground state itself, triaxial structures have typically been ascribed to pronounced γ softness, corresponding to a broad minimum in γ. This type of nuclei closely relates to the O(6) dynamical symmetry limit of the IBM-1, with the best known example being ^{196}Pt [6,17–19].

The low-spin spectra formed by a triaxial rigid rotor and a γ-soft nucleus exhibit rather similar features. Most important, the band head of the (quasi-)γ band is positioned at low energy, typically below the yrast-4^+ state. This is distinct from the

*mlettmann@ikp.tu-darmstadt.de

comparatively high energies of the γ band in axially symmetric rotors, which has also been discussed in neutron-rich Ar isotopes [20]. A significant difference between the soft and rigid cases is the energy spacing between the odd and even members of the γ band, i.e., the distance of the 3^+_γ state to the 2^+_γ and 4^+_γ states. In the case of a triaxial rigid rotor, the odd-spin levels are located closer to the lower-lying even spin levels, whereas the odd spin levels are closer to the higher-lying even spin levels in the case of a γ-soft nucleus. This relative location of even and odd spin states is usually referred as staggering [21,22]. The only experimental evidence in medium-heavy $A < 100$ nuclei for a significant degree of rigid triaxiality in the ground state was recently provided by Toh *et al.* [23] for the nucleus ^{76}Ge.

Besides the experimental confirmation of triaxiality in ^{76}Ge, various calculations were performed for even-even germanium isotopes from stability toward the magic neutron number $N = 50$. These calculations predict this region to be dominated by γ-soft nuclei with only one isolated case of a rigid triaxial deformed nucleus which is either ^{74}Ge [24–26] or ^{76}Ge [27]. Furthermore, it was shown that a new region of rigid triaxial deformation should arise around $N = 54$, which is supported by shell model and beyond-mean-field calculations [28,29], predicting a maximum of triaxiality for the exotic nucleus ^{86}Ge. Also in the broader mass region above $N = 50$, new Monte Carlo shell model calculations [30] predict the occurrence of coexisting prolate and triaxial shapes, e.g., leading to a low-lying triaxial band in ^{110}Zr at $N = 70$. For proton numbers between $Z = 28$ and 40, the $N = 56,58$ subshell closures ($2d_{5/2}$, $3s_{1/2}$) may diminish, possibly leading to the occurrence of triaxial structures at smaller values of N as compared to the chain of zirconium isotopes. Nevertheless, $N = 56,58$ may still have a stabilizing influence. The prediction of a region of triaxiality in neutron-rich germanium isotopes is backed by further systematic theoretical studies [31,32]. The present work aims at providing experimental benchmarks from γ-ray spectroscopy on the neutron-rich Ge isotopes up to $N = 56$.

At the Radioactive Isotope Beam Factory (RIBF), a ^{238}U beam with an energy of 345 MeV/u impinged on a 3-mm-thick ^{9}Be target at the entrance of the BigRIPS fragment separator [33]. The isotopes of interest were produced by in-flight fission, selected by the $B\rho$-ΔE-$B\rho$ method and identified on an event-by-event basis by the time of flight-$B\rho$-ΔE method in BigRIPS [34], in two different settings. ^{87}As and ^{85}Ge were obtained with rates of 2059 and 731 s^{-1}, respectively, for 22 h. For 10.5 h, ^{89}As was provided at a rate of 140 s^{-1}. The isotopes of interest impinged on the 99(1)-mm-thick liquid-hydrogen reaction target MINOS [35] at the end of BigRIPS. The ion's kinetic energy of ∼270 MeV/u was reduced by ∼70 MeV/u while passing the target. Products from secondary $(p,2p)$ or (p,pn) reactions in the LH_2 target were identified by the ZeroDegree spectrometer [33] applying the $B\rho$-ΔE-$B\rho$ method. Reaction vertices were determined by a time projection chamber (TPC) surrounding the LH_2 target. De-excitation γ rays were observed in the NaI(Tl) scintillator array DALI2 [36] covering polar angles from 10 to 128 deg with respect to the central beam axis and the center of MINOS. By a simulation within the GEANT4 framework [37], full-energy peak detection efficiencies of 35% (23%)

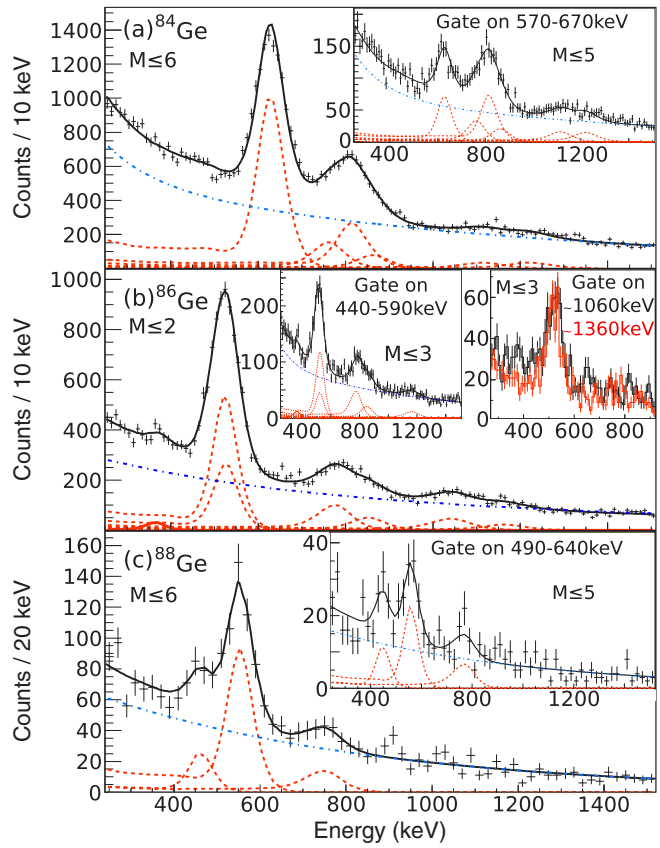

FIG. 1. DALI2 spectra obtained in the reactions (a) ^{85}Ge$(p,pn)^{84}$Ge, (b) ^{87}As$(p,2p)^{86}$Ge, and (c) ^{89}As$(p,2p)^{88}$Ge are shown as black data points, superimposed with the fit of the whole spectrum (black solid line). The respective background (blue dash-dotted line) and simulated response functions for each transition (red dotted and solid lines) are shown. Insets show spectra after gating on the 2^+_1 regions. In panel (b) also gates on the $2^+_2 \rightarrow 0^+_1$ (black) and a neighboring region (red) are shown. The multiplicity cutoff M for ^{86}Ge is chosen to optimize the background-to-peak balance according to available statistics. For ^{84}Ge higher, M is chosen to enhance higher-lying transitions and for ^{88}Ge because of the low statistics.

were obtained for a 500-keV (1-MeV) γ ray (with addback) emitted from a nucleus at the center of the target with a kinetic energy of 250 MeV/u. Energy calibrations were done with five transitions from ^{137}Cs, ^{88}Y, and ^{60}Co sources ranging from 662 keV to 1.836 MeV. A calibration error of 1.5 keV and an energy resolution of 9% (6%) FWHM at 662 keV (1.332 MeV) was obtained, in agreement with the analyses from Refs. [36,38,39].

The Doppler-corrected γ-ray spectra of ^{84,86,88}Ge are shown in Fig. 1. Each energy spectrum is described by a least-squares fit based on spectral response functions and line shapes obtained from Monte Carlo simulations, and a two-component exponential background. Derived transition energies have errors consisting of three contributions: the uncertainty of the energy calibration, the statistical error from the fitting procedure, and an error arising from the lifetime-dependent Doppler broadening and shift of the observed line shapes.

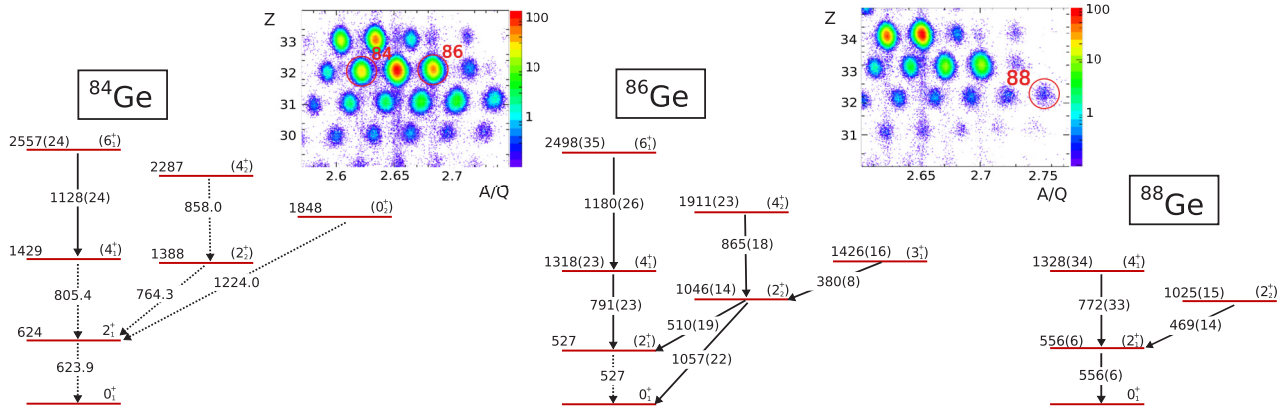

FIG. 2. Measured transition energies and proposed level energies of ^{84,86,88}Ge. Dashed arrows denote transition energies taken from literature [40–43] and solid arrows mark transitions measured for the first time. The tentative spin assignments for ^{84}Ge are taken from Ref. [40] (see text). In addition, ZeroDegree-ID plots from the outgoing channel for both settings are shown. The corresponding germanium isotopes are marked with circles.

Upper limits of the lifetimes were derived by a χ^2 analysis. The derived upper limits are compatible with suggestions from the applied theories (see below).

^{84}Ge was populated by the ^{85}Ge(p,pn) reaction and, with a number of known γ rays from β-delayed spectroscopy [40–42] served as a check for the spectral analysis. Six transitions at energies of 629(7), 772(18), 813(10), 867(13), 1128(24), and 1229(15) keV were identified [see Fig. 1(a)], the 1128-keV transition for the first time. The other five transitions are in good agreement with Ref. [40], and a proposed level scheme is shown in Fig. 2. The present experiment is not sensitive to the spins of the involved states. However, based on systematics in neighboring Ge isotopes, we assign the newly observed 1128(24)-keV γ ray to the $(6_1^+) \rightarrow 4_1^+$ transition. The inset of Fig. 1(a) shows the result of a coincidence condition on the $2_1^+ \rightarrow 0_1^+$ transition. The 629(7)-keV transition still appears due to coincidences with Compton events of higher-energy transitions underneath the 629(7)-keV peak, but is largely reduced.

^{86}Ge was populated by the ^{87}As$(p,2p)$ reaction, and the obtained Doppler-corrected spectrum is shown in Fig. 1(b). Seven transitions at energies 380(8), 510(19), 534(8), 791(23), 865(18), 1057(22), and 1180(26) keV were measured. Only the 534(8)-keV transition has formerly been observed following β decay [43] and assigned to the decay of the (2_1^+) state, in agreement with the present data. A proposed level scheme of ^{86}Ge is presented in Fig. 2, based on the following observations. For even-even nuclei populated in $(p,2p)$ reactions (see, e.g., Refs. [44–47]), the strongest observed γ decay in the spectrum stems from the transition $(2_1^+) \rightarrow 0_1^+$, while the second strongest intensity typically originates from the $(4_1^+) \rightarrow (2_1^+)$ transition. The inset in Fig. 1(b) displays a $\gamma\gamma$-coincidence spectrum, gated on the energy range from 440 to 590 keV. A strong peak in the gated energy range remains due to the 510(19)/534(8)-keV doublet. The peak at 1057(22) keV is not in coincidence with the gated energy range. We assign this transition as the ground-state transition of a 2^+ state at 1057(22) keV. The fitted energies of the doublet, 510(19) and 534(8) keV, sum up to 1057(22) keV within error. Therefore, we assign the 510(19)-keV γ ray to the $(2_2^+) \rightarrow (2_1^+)$ transition. The transitions at 865(18) and 1180(26) keV are assigned to be $(4_2^+) \rightarrow (2_2^+)$ and $(6_1^+) \rightarrow (4_1^+)$, respectively, based on comparison to ^{84}Ge. A standard significance test [48] for the 380-keV peak yields $\sim 4\sigma$ in singles and $>2\sigma$ in the gated spectra. This transition appears in the gate on the $\sim$520-keV doublet, and weakly in the gate on the 1060-keV region where the $(2_2^+) \rightarrow (0_1^+)$ transition is found. A gate on a neighboring ($\sim$1360-keV) region yields no 380-keV peak [see Fig. 1(b)]. As discussed further below, this transition is tentatively assigned to the $(3_1^+) \rightarrow (2_2^+)$ transition.

The Doppler-corrected γ spectrum from the reaction ^{89}As$(p,2p)^{88}$Ge is shown in Fig. 1(c). The three γ-ray transitions at energies 469(14), 556(6), and 772(33) keV are observed for the first time. A suggested level scheme of ^{88}Ge is presented in Fig. 2. The transition at 556(6) keV has the strongest intensity, indicating a $(2_1^+) \rightarrow 0_1^+$ transition. The γ ray at 772(33) keV is assigned to the $(4_1^+) \rightarrow (2_1^+)$ transition, and the γ ray at 469(14) keV is assigned to the $(2_2^+) \rightarrow (2_1^+)$ transition from comparison to neighboring ^{86}Ge and ^{90}Se [49]. A gate on the $2_1^+ \rightarrow 0_1^+$ transition [see inset of Fig. 1(c)] yields both transitions.

The trends of the 2_1^+ energies for even-even nuclei from Zr ($Z = 40$) to Ge ($Z = 32$) are depicted in Fig. 3(a). In zirconium isotopes, the 2_1^+ energy peaks at $N = 56$. It maintains a rather high value at $N = 58$ before it significantly drops at the onset of collectivity at $N = 60$. For Sr [50–54,56], Kr [50–53,56,57], and Se [49,57,59] isotopes, no such peaking of the 2_1^+ energies is found, but rather a flat behavior up to $N = 58$. Nevertheless, a slight increase in the 2_1^+ energy at $N = 56$ is observed for ^{92}Kr and ^{88}Ge (this work). The corresponding ratios $R_{4/2} = E(4_1^+)/E(2_1^+)$ are shown in Fig. 3(b). The systematic trend in the Ge isotopic chain is similar to those in the Kr and Se isotopic chains, but significantly different from the Zr and Sr isotopic chains. An increase of $R_{4/2}$ from $N = 50$ to $N = 54$, followed by a drop toward $N = 56$, is observed. Usually, an increase of collectivity is mirrored by a drop of 2_1^+ energies and a rise of $R_{4/2}$ towards the rotational limits. The flat behavior of 2_1^+

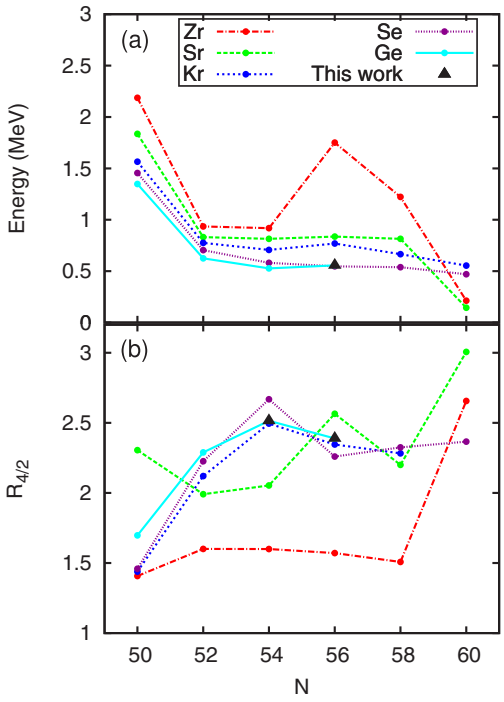

FIG. 3. (a) Behavior of the 2_1^+ energies for the isotopic chains of Zr ($Z = 40$) [50–55], Sr ($Z = 38$) [50–54,56], Kr ($Z = 36$) [50–53,56–58], Se ($Z = 34$) [49,57,59], and Ge ($Z = 32$) [40–43,57,60]. (b) Trend of the $R_{4/2}$ ratios of the same isotopic chains.

energies from $Z = 38$ (Sr) down to $Z = 32$ (Ge), along with the $R_{4/2}$ trend, may therefore indicate a remnant of the $N = 56$ subshell closure driving ^{88}Ge somewhat back to sphericity, or a small fluctuation in their collective structure. All ^{84,86,88}Ge isotopes have $R_{4/2}$ ratios around 2.5, which is typical for nuclei with triaxial features.

In the following, the experimental results are compared to shell-model calculations and a symmetry-conserving configuration mixing Gogny (SCCM) calculation. For more details on these calculations, and including a shell-model calculation for ^{84}Ge, we refer to Ref. [28] and references therein. In Fig. 4, the level schemes of ^{86,88}Ge are compared to the predictions from both theories. The predicted sequences of the states are in good agreement with the proposed ones from data, although excitation energies are overestimated in all cases. For both nuclei the predicted $R_{4/2}$ ratios of ∼2.5 agree with the data. The low-lying γ band in both sets of calculations reflects a degree of triaxiality in both isotopes. This is shown by the $R_{4/2}$ and $R_{2/2} = E(2_2^+)/E(2_1^+)$ ratios given in Table I. Furthermore, both theories predict a 3_1^+ state which is closer to the 2_2^+ state

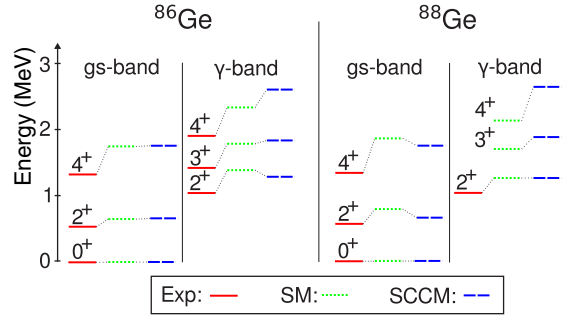

FIG. 4. Systematics of the ^{86,88}Ge level energies from experiment compared to theoretical predictions from shell model (SM) and SCCM.

than to the 4_2^+ state in the γ band (except for the rather centered position in case of the ^{88}Ge shell-model calculation). This is especially the case for ^{86}Ge. A promising candidate for this state in ^{86}Ge is observed in the present experiment through the 380(8)-keV transition, since the strongest decay from the 3_1^+ state is expected to be to the 2_2^+ state. Although an excited 0^+ state is predicted in this energy range, we stress that it would dominantly decay to the 2_1^+ state. In the present experiment, such a $(0^+) \rightarrow 2_1^+$ transition is observed only for ^{84}Ge, but not for ^{86}Ge where it would be located at 899 keV. This disfavors a $J = 0$ assignment and leads to the tentative $J = 3$ assignment.

The staggering in the γ band [21]

$$S(J) = \frac{[E(J) - E(J-1)] - [E(J-1) - E(J-2)]}{E(2_1^+)} \tag{1}$$

should take a positive value for $J = 4$ for a rigid triaxial nucleus. Note that this will trivially be the case also for a well-deformed rotor with $E(J) \propto J(J+1)$. However, in such a case the position of the γ bandhead is much higher relative to the yrast states. The same argument can be made for known realizations of spherical-deformed transitional nuclei. In the only known case of a nucleus in the medium-heavy mass region $A < 100$ with rigid triaxial deformation in the ground state, ^{76}Ge [23], $S(4) = 0.091(2)$ has been found. With the present assignments for ^{86}Ge a value of $S(4) = 0.20(4)$ results, pointing at an even larger degree of triaxiality in the ground state. The experimental $S(4)$ agrees with the results obtained from both theories, shown in Table I. There are strong similarities in the level schemes of ^{86}Ge and ^{76}Ge (see Fig. 5); the level energies agree within 100 keV. Especially the relative positions of the odd- to the even-spin γ-band members are consistent. This matches very well the predictions from

TABLE I. Comparison of experimental and theoretical $R_{4/2}$, $R_{2/2}$, and $S(4)$.

	^{84}Ge		^{86}Ge			^{88}Ge			Rigid triaxial
	Expt.	SM	Expt.	SM	SCCM	Expt.	SM	SCCM	rotor
$R_{4/2}$	2.290(4)	2.08	2.50(4)	2.69	2.66	2.39(7)	2.37	2.66	2.67
$R_{2/2}$	2.224(4)	2.05	1.98(3)	2.14	1.95	1.84(3)	1.60	1.92	2
$S(4)$		−0.52	0.20(4)	0.23	0.33		−0.01	0.22	1.67

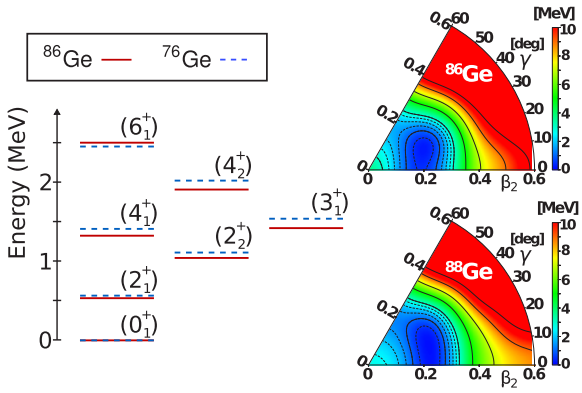

FIG. 5. (Left) Comparison of the low spin spectrum of ^{76}Ge (blue, dashed) and ^{86}Ge (red, solid). (Right) Potential energy surfaces in the particle number variation after projection (PN-VAP) approach [64] for ^{86}Ge (top) and ^{88}Ge (bottom). The spacing between solid contour lines is 2 MeV with intermediate dashed lines for 0.5-MeV steps. The minima are located about $\beta_2 = 0.2$.

both models considered, shell model and SCCM (see Fig. 4). Examining the potential energy surfaces from the SCCM calculations (see Fig. 5), a triaxial minimum is found for ^{86}Ge, and ^{88}Ge is predicted to be very similar, with a somewhat larger β deformation and more γ softness. Interestingly, the shell model yields a smaller $R_{4/2}$ ratio for ^{88}Ge than for ^{86}Ge (see Table I), which may reflect the effect of the $N = 56$ subshell closure in the calculation. In both SCCM calculations, the wave functions of the low-lying states maximize at triaxial values. Similar conclusions are drawn from the shell-model calculations. From an analysis of $E2$ matrix elements, i.e., the use of quadrupole shape invariants [61], we derive an invariant K_3 of 0.027 for both, ^{86,88}Ge, in the SCCM, corresponding to an effective γ value of 29.5° near maximum triaxiality. However, the fluctuations of K_3 are very different for ^{86,88}Ge, that is, 0.01 and 0.13, respectively, which reflects the large degree of triaxial rigidity in ^{86}Ge. Similarly, the shell model yields large triaxiality for both isotopes, and fluctuations in K_3 are an order of magnitude larger in ^{88}Ge than in ^{86}Ge. We note that different cutoffs in the sums for deriving the shape invariants give consistent results, similar to previous works [62,63].

To conclude, γ spectroscopy of neutron-rich Ge isotopes has been performed, for the first time with ^{88}Ge. In total, 16 transitions in ^{84,86,88}Ge have been observed, 10 of which were so far unknown. On the basis of the observed intensities and systematics in neighboring Ge isotopes, new level schemes for ^{86,88}Ge are proposed for the first time. The tentative assignment of a 3^+_1 state in ^{86}Ge would be compatible to new model predictions, as well as to typical collective-model level orderings. This points to a degree of rigid triaxiality in this nucleus, which has previously been predicted within this broader mass region. New calculations predict a maximum of triaxiality in ^{86}Ge. Our measurements show the first indication of rigid ground-state triaxiality in this very neutron-rich region of the nuclear chart. ^{86}Ge may constitute the first example of an unstable nucleus with this feature in this newly accessible region, which is much discussed in view of triaxial features, as well as shape coexistence. Hence, future more detailed studies of ^{86}Ge are highly desirable. A study of Effective Single-Particle Energies (ESPEs) like in ^{110}Zr [30] may shed light on the possibility of the emergence of triaxiality as the result of the bunching of single-particle orbitals.

The authors thank the RIBF and BigRIPS teams for providing a stable, high-intensity uranium beam and operating the secondary beams. We acknowledge support from the German BMBF Grants No. 05P15RDFN1, No. 05P12RDFN8, and No. 05P15PKFNA; ERC Grant No. MINOS-258567; the Spanish Ministerio de Economía y Competitividad under Contracts No. FPA2014-57196-C5-4-P and No. FIS-2014-53434, the Vietnam Ministry of Science and Technology, as well as from the Science and Technology Facilities Council (STFC). We further thank GSI for providing computing facilities.

[1] A. Bohr and B. Mottelson, Mat. Fys. Medd. Dan. Vid. Selsk. **27** (1953).
[2] A. S. Davydov and G. F. Filippov, Nucl. Phys. **8**, 237 (1958).
[3] L. Wilets and M. Jean, Phys. Rev. **102**, 788 (1956).
[4] M. Göppert-Mayer, Phys. Rev. **75**, 1969 (1949).
[5] M. Göppert-Mayer and J. H. D. Jensen, *Elementary Theory of Nuclear Shell Structure* (Wiley, New York, 1955).
[6] F. Iachello and A. Arima, *The Interacting Boson Model* (Cambridge University Press, Cambridge, UK, 1987).
[7] M. Bender, P.-H. Heenen, and P.-G. Reinhard, Rev. Mod. Phys. **75**, 121 (2003).
[8] T. R. Rodríguez and J. L. Egido, Phys. Rev. C **81**, 064323 (2010).
[9] S. W. Ødegård, G. B. Hagemann, D. R. Jensen, M. Bergström, B. Herskind, G. Sletten, S. Törmänen, J. N. Wilson, P. O. Tjøm, I. Hamamoto *et al.*, Phys. Rev. Lett. **86**, 5866 (2001).
[10] D. J. Hartley, R. V. F. Janssens, L. L. Riedinger, M. A. Riley, A. Aguilar, M. P. Carpenter, C. J. Chiara, P. Chowdhury, I. G. Darby, U. Garg *et al.*, Phys. Rev. C **80**, 041304(R) (2009).
[11] G. Schonwasser, H. Hubel, G. B. Hagemann, P. Bednarczyk, G. Benzoni, A. Bracco, P. Bringel, R. Chapman, D. Curien, J. Domscheit *et al.*, Phys. Lett. B **552**, 9 (2003).
[12] S. Frauendorf and J. Meng, Nucl. Phys. A **617**, 131 (1997).
[13] T. Koike, K. Starosta, and I. Hamamoto, Phys. Rev. Lett. **93**, 172502 (2004).
[14] K. Starosta, T. Koike, C. J. Chiara, D. B. Fossan, and D. R. LaFosse, Nucl. Phys. A **682**, 375 (2001).
[15] A. D. Ayangeakaa, U. Garg, M. D. Anthony, S. Frauendorf, J. T. Matta, B. K. Nayak, D. Patel, Q. B. Chen, S. Q. Zhang, P. W. Zhao *et al.*, Phys. Rev. Lett. **110**, 172504 (2013).
[16] D. Tonev, G. de Angelis, P. Petkov, A. Dewald, S. Brant, S. Frauendorf, D. L. Balabanski, P. Pejovic, D. Bazzacco, P. Bednarczyk *et al.*, Phys. Rev. Lett. **96**, 052501 (2006).

[17] J. A. Cizewski, R. F. Casten, G. J. Smith, M. L. Stelts, W. R. Kane, H. G. Börner, and W. F. Davidson, Phys. Rev. Lett. **40**, 167 (1978).
[18] J. Jolie, J. M. Régis, D. Wilmsen, N. Saed-Samii, M. Pfeiffer, N. Warr, A. Blanc, M. Jentschel, U. Köster, P. Mutti *et al.*, Nucl. Phys. A **934**, 1 (2015).
[19] N. Pietralla, T. Möller, C. J. Lister, E. A. McCutchan, G. Rainovski, C. Bauer, M. P. Carpenter, R. V. F. Janssens, D. Seweryniak, and S. Zhu, EPJ Web Conf. **93**, 01002 (2015).
[20] S. Bhattacharyya, M. Rejmund, A. Navin, E. Caurier, F. Nowacki, A. Poves, R. Chapman, D. O'Donnell, M. Gelin, A. Hodsdon *et al.*, Phys. Rev. Lett. **101**, 032501 (2008).
[21] N. V. Zamfir and R. F. Casten, Phys. Lett. B **260**, 265 (1991).
[22] E. A. McCutchan, D. Bonatsos, N. V. Zamfir, and R. F. Casten, Phys. Rev. C **76**, 024306(R) (2007).
[23] Y. Toh, C. J. Chiara, E. A. McCutchan, W. B. Walters, R. V. F. Janssens, M. P. Carpenter, S. Zhu, R. Broda, B. Fornal, B. P. Kay *et al.*, Phys. Rev. C **87**, 041304(R) (2013).
[24] S. F. Shen, S. J. Zheng, F. R. Xu, and R. Wyss, Phys. Rev. C **84**, 044315(R) (2011).
[25] J. J. Sun, Z. Shi, X. Q. Li, H. Hua, C. Xu, Q. B. Chen, S. Q. Zhang, C. Y. Song, J. Meng, X. G. Wu *et al.*, Phys. Lett. B **734**, 308 (2014).
[26] T. Nikšić, P. Marević, and D. Vretenar, Phys. Rev. C **89**, 044325 (2014).
[27] D.-L. Zhang and B.-G. Ding, Chin. Phys. Lett. **30**, 122101(R) (2013).
[28] K. Sieja, T. R. Rodríguez, K. Kolos, and D. Verney, Phys. Rev. C **88**, 034327(R) (2013).
[29] M. Lebois, D. Verney, F. Ibrahim, S. Essabaa, F. Azaiez, M. Cheikh Mhamed, E. Cottereau, P. V. Cuong, M. Ferraton, K. Flanagan *et al.*, Phys. Rev. C **80**, 044308(R) (2009).
[30] T. Togashi, Y. Tsunoda, T. Otsuka, and N. Shimizu, Phys. Rev. Lett. **117**, 172502 (2016).
[31] L. Guo, J. A. Maruhn, and P.-G. Reinhard, Phys. Rev. C **76**, 034317(R) (2007).
[32] S. Hilaire and M. Girod, *Cea* http://www-phynu.cea.fr
[33] T. Kubo, D. Kameda, H. Suzuki, N. Fukuda, H. Takeda, Y. Yanagisawa, M. Ohtake, K. Kusaka, K. Yoshida, N. Inabe *et al.*, Prog. Theor. Exp. Phys. **2012**, 03C003 (2012).
[34] N. Fukuda, T. Kubo, T. Ohnishi, N. Inabe, H. Takeda, D. Kameda, and H. Suzuki, Nucl. Instrum. Methods Phys. Res., Sect. B **317**, 323 (2013).
[35] A. Obertelli, A. Delbart, S. Anvar, L. Audirac, G. Authelet, H. Baba, B. Bruyneel, D. Calvet, F. Château, A. Corsi *et al.*, Eur. Phys. J. A **50**, 8 (2014).
[36] S. Takeuchi, T. Motobayashi, Y. Togano, M. Matsushita, N. Aoi, K. Demichi, H. Hasegawa, and H. Murakami, Nucl. Instrum. Methods Phys. Res., Sect. A **763**, 596 (2014).
[37] S. Agostinelli, J. Allison, K. Amako, J. Apostolakis, H. Araujo, P. Arce, M. Asai, D. Axen, S. Banerjee, G. Barrand *et al.*, Nucl. Instrum. Methods Phys. Res., Sect. A **506**, 250 (2003).
[38] P. Doornenbal, Prog. Theor. Exp. Phys. **2012**, 03C004 (2012).
[39] C. Santamaria, C. Louchart, A. Obertelli, V. Werner, P. Doornenbal, F. Nowacki, G. Authelet, H. Baba, D. Calvet, F. Château *et al.*, Phys. Rev. Lett. **115**, 192501 (2015).
[40] A. Korgul, K. P. Rykaczewski, R. Grzywacz, H. Śliwińska, J. C. Batchelder, C. Bingham, I. N. Borzov, N. Brewer, L. Cartegni, A. Fijałkowska *et al.*, Phys. Rev. C **88**, 044330 (2013).
[41] K. Kolos, D. Verney, F. Ibrahim, F. Le Blanc, S. Franchoo, K. Sieja, F. Nowacki, C. Bonnin, M. Cheikh Mhamed, P. V. Cuong *et al.*, Phys. Rev. C **88**, 047301 (2013).
[42] J. A. Winger, K. P. Rykaczewski, C. J. Gross, R. Grzywacz, J. C. Batchelder, C. Goodin, J. H. Hamilton, S. V. Ilyushkin, A. Korgul, W. Królas *et al.*, Phys. Rev. C **81**, 044303 (2010).
[43] K. Miernik, K. P. Rykaczewski, C. J. Gross, R. Grzywacz, M. Madurga, D. Miller, J. C. Batchelder, I. N. Borzov, N. T. Brewer, C. Jost *et al.*, Phys. Rev. Lett. **111**, 132502 (2013).
[44] P. Doornenbal, H. Scheit, S. Takeuchi, N. Aoi, K. Li, M. Matsushita, D. Steppenbeck, H. Wang, H. Baba, H. Crawford *et al.*, Phys. Rev. Lett. **111**, 212502 (2013).
[45] H. Iwasaki, A. Lemasson, C. Morse, A. Dewald, T. Braunroth, V. M. Bader, T. Baugher, D. Bazin, J. S. Berryman, C. M. Campbell *et al.*, Phys. Rev. Lett. **112**, 142502 (2014).
[46] D. Bazin, B. A. Brown, C. M. Campbell, J. A. Church, D. C. Dinca, J. Enders, A. Gade, T. Glasmacher, P. G. Hansen, W. F. Mueller *et al.*, Phys. Rev. Lett. **91**, 012501 (2003).
[47] P. Fallon, E. Rodriguez-Vieitez, A. O. Macchiavelli, A. Gade, J. A. Tostevin, P. Adrich, D. Bazin, M. Bowen, C. M. Campbell, R. M. Clark *et al.*, Phys. Rev. C **81**, 041302 (2010).
[48] K. Weise, K. Hübel, E. Rose, M. Schläger, D. Schrammel, M. Täschner, and R. Michel, Radiat. Prot. Dosimetry **121**, 52 (2006).
[49] S. Chen, P. Doornenbal, A. Obertelli, T. R. Rodríguez, G. Authelet, H. Baba, D. Calvet, F. Château, A. Corsi, A. Delbart *et al.*, Phys. Rev. C **95**, 041302(R) (2017).
[50] E. Browne, Nucl. Data Sheets **82**, 379 (1997).
[51] C. M. Baglin, Nucl. Data Sheets **113**, 2187 (2012).
[52] D. Abriola and A. A. Sonzogni, Nucl. Data Sheets **107**, 2423 (2006).
[53] D. Abriola and A. A. Sonzogni, Nucl. Data Sheets **109**, 2501 (2008).
[54] B. Singh and Z. Hu, Nucl. Data Sheets **98**, 335 (2003).
[55] B. Singh, Nucl. Data Sheets **109**, 297 (2008).
[56] E. A. Mccutchan and A. A. Sonzogni, Nucl. Data Sheets **115**, 135 (2014).
[57] A. Negret and B. Singh, Nucl. Data Sheets **124**, 1 (2015).
[58] M. Albers, N. Warr, K. Nomura, A. Blazhev, J. Jolie, D. Mücher, B. Bastin, C. Bauer, C. Bernards, L. Bettermann *et al.*, Phys. Rev. Lett. **108**, 062701 (2012).
[59] A. A. Sonzogni, M. Fadil, and B. Pfeiffer, Nucl. Data Sheets **110**, 2815 (2009).
[60] J. K. Tuli, Nucl. Data Sheets **98**, 209 (2003).
[61] V. Werner, N. Pietralla, P. von Brentano, R. F. Casten, and R. V. Jolos, Phys. Rev. C **61**, 021301 (2000).
[62] V. Werner, P. von Brentano, and R. V. Jolos, Phys. Lett. B **521**, 146 (2001).
[63] V. Werner, C. Scholl, and P. von Brentano, Phys. Rev. C **71**, 054314 (2005).
[64] M. Anguiano, J. Egido, and L. Robledo, Phys. Lett. B **545**, 62 (2002).